Kent Academic Repository
Full text document (pdf)

Mass flow measurement of gas-liquid two-phase CO_2 in CCS transportation pipelines using Coriolis flowmeters

Lijuan Wang[a,b], Yong Yan[b,*], Xue Wang[c], Tao Wang[d], Quansheng Duan[a], Wenbiao Zhang[a]

[a] *School of Control and Computer Engineering, North China Electric Power University, Beijing 102206, China*
[b] *School of Engineering and Digital Arts, University of Kent, Canterbury, Kent CT2 7NT, UK*
[c] *School of Mathematics, Statistics and Actuarial Science, University of Kent, Canterbury, Kent CT2 7NF, UK*
[d] *KROHNE Ltd., 34-38 Rutherford Drive, Wellingborough, NN8 6AE, UK*

ARTICLE INFO

ABSTRACT

Carbon Capture and Storage (CCS) is a promising technology that stops the release of CO_2 from industrial processes such as electrical power generation. Accurate measurement of CO_2 flows in a CCS system where CO_2 flow is a gas, liquid, or gas-liquid two-phase mixture is essential for the fiscal purpose and potential leakage detection. This paper presents a novel method based on Coriolis mass flowmeters in conjunction with least squares support vector machine (LSSVM) models to measure gas-liquid two-phase CO_2 flow under CCS conditions. The method uses a classifier to identify the flow pattern and individual LSSVM models for the metering of CO_2 mass flowrate and prediction of gas volume fraction of CO_2, respectively. Experimental work was undertaken on a multiphase CO_2 flow test facility. Performance comparisons between the general LSSVM and flow pattern based LSSVM models are conducted. Results demonstrate that Coriolis mass flowmeters with the LSSVM model incorporating flow pattern identification algorithms perform significantly better than those using the general LSSVM model. The mass flowrate measurement of gas-liquid CO_2 is found to yield errors less than $\pm$ 2% on the horizontal pipeline and $\pm$ 1.5% on the vertical pipeline, respectively, over flowrates from 250 kg/h to 3200 kg/h. The error in the estimation of CO_2 gas volume fraction is within $\pm$ 10% over the same range of flow rates.

1. Introduction

Accurate measurement of CO_2 is essential in the practical deployment of the carbon capture and storage (CCS) technology. Pipeline networks are regarded as the most effective solution to the long distance onshore transportation of CO_2 from capture facilities to storage sites. However, the measurement of CO_2 flow in CCS pipelines is more challenging than metering the oil, gas or multiphase flow in the air and gas industry due to the readily varying physical properties of CO_2. The phase boundaries in the CO_2 phase diagram are close to each other and under ambient conditions. In this case, unstable temperature or pressure of CO_2 flow may result in significant variations in the CO_2 physical characteristics (Hunter and Leslie, 2009). In addition, presence of impurities such as N_2 and CH_4 may also affect the phase properties of CO_2 flow. It is thus challenging to accurately measure and subsequently control CO_2 flows in CCS pipelines. Orifice plate flowmeters and turbine flowmeters have been applied for general single-phase CO_2 measurement in tertiary recovery projects for some years (Hunter and Leslie, 2009). However, it is reported that the Orifice flowmeters for the

measurement of slugging gas-liquid flow at the well-head generate the maximum error of 80% (Green et al., 2008). Coriolis mass flowmeters are capable of directly metering mass flowrate of the fluid regardless of its physical state and providing density and temperature. Application of Coriolis mass flowmeters to the measurement of single-phase gas/liquid CO_2 flow have been conducted (Adefila et al., 2015; Adefila et al., 2017; Lin et al., 2014). Recently, Coriolis flowmeters in conjunction with a theoretical bubble-effect equation, a trained neural network and a fuzzy inference system with additional flow sensing devices were proposed to measure air-water flow (Wang and Baker, 2014; Kunze et al., 2014; Hemp and Sultan, 1989; Liu et al., 2001; Safarinejadian et al., 2012; Hou et al., 2014; Xing et al., 2014; Wang et al., 2017a,b). However, CO_2 two-phase flow is more challenging to measure compared to air-water flow due to the transitions between different phases depending on the environmental conditions. Although a Coriolis mass flowmeter with a neural network model was evaluated with slugging gas-liquid CO_2 flow, the error was found up to $\pm$ 5% (Green et al., 2008). However, the gas component of the CO_2 flow was not measured and the impact of different flow regimes was not considered. Moreover, significant

challenges are to overcome for the direct flow measurement techniques to achieve 1.5% measurement uncertainty specified in the European Union − Emissions Trading Scheme under all expected CCS conditions (TUV NEL, 2009).

In this study, Coriolis mass flowmeters (KROHNE OPTIMASS 6400 S15) are applied to measure gas-liquid CO_2 flow with different flow regimes and their performance evaluated under a range of CCS conditions. This paper aims to assess the effect of flow regimes on the performance of Coriolis mass flowmeters and improve the measurement accuracy of the total CO_2 mass flowrate and CO_2 gas volume fraction under two-phase flow conditions. An FP_LSSVM (Flow Pattern based Least Squares Support Vector Machine) model is developed to identify the flow regime and then measure CO_2 mass flowrate and gas volume fraction. For purpose of a direct comparison, a general LSSVM model is also developed with the same experimental data covering different flow regimes. The LSSVM and FP_LSSVM models are compared in terms of measurement accuracy under a range of flow conditions.

2. Methodology

2.1. Flow pattern based data-driven model

The flow pattern based data-driven model, as shown in Fig. 1, includes a model for flow pattern identification and individual correction model for CO_2 mass flowrate and prediction model for CO_2 gas volume fraction. The Coriolis mass flowmeter provides apparent mass flowrate and observed density of the two-phase fluid by analyzing the internal vibration signals from the measuring tubes. Despite that the apparent mass flowrate and observed density from the flowmeter are erroneous under two-phase flow conditions (unlike under single-phase flow conditions), these two parameters still reflect the variations in the actual CO_2 mass flowrate and gas quantity. The outputs of the Coriolis mass flowmeter and the differential pressure (DP) transducer are applied to identify the flow pattern and then the corresponding correction and prediction models are selected to yield corrected CO_2 mass flowrate and estimated gas volume fraction.

The flow pattern identification model is in effect a classifier whilst the correction and prediction models act as regression functions. In this study, the data-driven models are developed based on LSSVM which is a least squares version of support vector machine. This modified SVM (Suykens and Vandewalle, 1999) incorporating the least squares procedure obtains the optimal solution through solving a set of linear equations instead of a convex quadratic programming problem in the classical SVM. As a result, the computational complexity of LSSVM is significantly reduced, when compared to SVM (Huang et al., 2012).

2.2. LSSVM model for classification

The basic idea of SVM for solving a two-class classification problem is to map the data into a high-dimensional space and then construct an optimal separating hyperplane in this space (Cortes and Vapnik, 1995). Instead of solving a quadratic programming problem, equality constraints for the classification problem have been considered. As a result, the optimization problem is simplified to resolve several linear

equations (Suykens and Vandewalle, 1999). Given n training samples $\mathbf{X}^* = (\mathbf{x}_1, \mathbf{x}_2, ..., \mathbf{x}_n)$ and the desired output $\mathbf{y}$, each input sample is a vector $\mathbf{x} = (x_1, x_2, ..., x_m)^T$ including m variables. The term $\frac{2}{\|\omega\|}$ is defined as the distance between the two different classes in the feature space, where ω is a weight vector. To maximize the separating margin and to minimize the training error is equivalent to

$$\min_{\omega,e,b} \frac{1}{2}\|\omega\|^2 + \gamma\frac{1}{2}\sum_{i=1}^{n} e_i^2$$

s.t. $y_i(\langle\omega, \varphi(\mathbf{x}_i)\rangle + b) = 1 - e_i$, $i = 1, ..., n$ \hfill (1)

where γ is a penalty parameter that balances model complexity and approximation accuracy, e_i is the ith error variable and b is a bias. $\varphi(\mathbf{x}_i)$ is a nonlinear function which maps the data into the feature space. The Lagrangian function is given by:

$$L = \frac{1}{2}\|\omega\|^2 + \gamma\frac{1}{2}\sum_{i=1}^{n} e_i^2 - \sum_{i=1}^{n} \alpha_i[y_i(<\omega, \varphi(\mathbf{x}_i)> + b) - 1 + e_i]$$
\hfill (2)

where α_i ($i = 1, ..., n$) are Lagrange multipliers. The optimality conditions for Eq. (2) are refined as:

$$\begin{cases} \frac{\partial L}{\partial \omega} & = 0 \rightarrow \omega = \sum_{i=1}^{n} \alpha_i y_i \varphi(\mathbf{x}_i) \\ \frac{\partial L}{\partial b} & = 0 \rightarrow \sum_{i=1}^{n} \alpha_i y_i = 0 \\ \frac{\partial L}{\partial e_i} & = 0 \rightarrow \alpha_i = \gamma e_i \\ \frac{\partial L}{\partial \alpha_i} & = 0 \rightarrow y_i(<\omega, \varphi(\mathbf{x}_i)> + b) - 1 + e_i = 0 \end{cases}$$
\hfill (3)

Eq. (3) can be written as the solution to the following set of linear equations:

$$\begin{bmatrix} \mathbf{I} & 0 & 0 & -\mathbf{Z}^T \\ 0 & 0 & 0 & -\mathbf{y}^T \\ 0 & 0 & \gamma\mathbf{I} & -\mathbf{I} \\ \mathbf{Z} & \mathbf{y} & \mathbf{I} & 0 \end{bmatrix}\begin{bmatrix} \omega \\ b \\ e \\ \alpha \end{bmatrix} = \begin{bmatrix} 0 \\ 0 \\ 0 \\ \mathbf{1}_v \end{bmatrix}$$
\hfill (4)

where $Z = (\varphi(\mathbf{x}_i)^T y_1, ..., \varphi(\mathbf{x}_n)^T y_n)^T$, $y = (y_1, ..., y_n)^T$, $\mathbf{1}_v = (1, ..., 1)^T$, $\mathbf{e} = (e_1, ..., e_n)^T$, , $\mathbf{I}$ is an $n \times n$ identity matrix. The two terms of α and b can be resolved by

$$\begin{bmatrix} 0 & -\mathbf{y}^T \\ \mathbf{y} & ZZ^T + I/\gamma \end{bmatrix}\begin{bmatrix} b \\ \alpha \end{bmatrix} = \begin{bmatrix} 0 \\ 1_v \end{bmatrix}$$
\hfill (5)

Mercer's condition can be used to the matrix $\mathbf{H} = \mathbf{ZZ}^T$, where

$$\mathbf{H}_{i,k} = y_i y_k \varphi(\mathbf{x}_i)^T \varphi(\mathbf{x}_k) = y_i y_k K(\mathbf{x}_i, \mathbf{x}_k)$$
$$i, k = 1, ..., n$$
\hfill (6)

$K(\mathbf{x}_i, \mathbf{x}_k)$ represents a kernel function. The decision function of the two-class classifier is described as

$$y = f(\mathbf{x}) = sign\left(\sum_{i=1}^{n} \alpha_i y_i K(\mathbf{x}, \mathbf{x}_i) + b\right)$$
\hfill (7)

The kernel function $K(\mathbf{x}, \mathbf{x}_i)$ used to develop the LSSVM models in this study is RBF (Radial Basis Function), which is defined as:
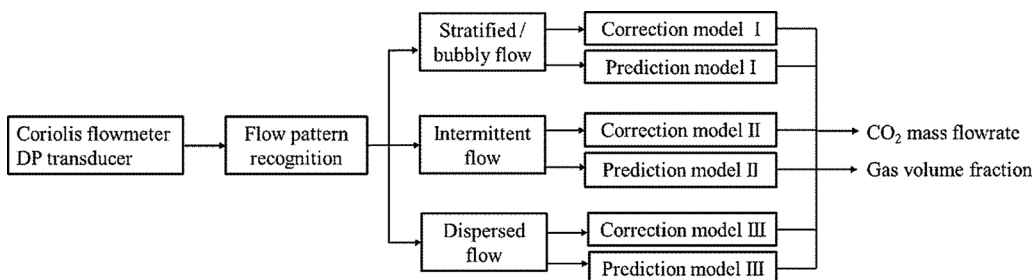

Fig. 1. Principle of the flow pattern based model for mass flow metering and gas volume fraction predication on horizontal or vertical pipes.
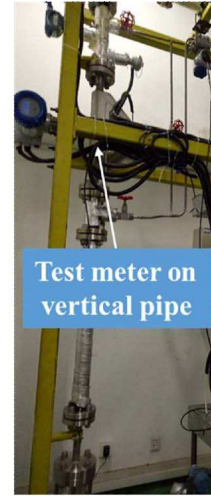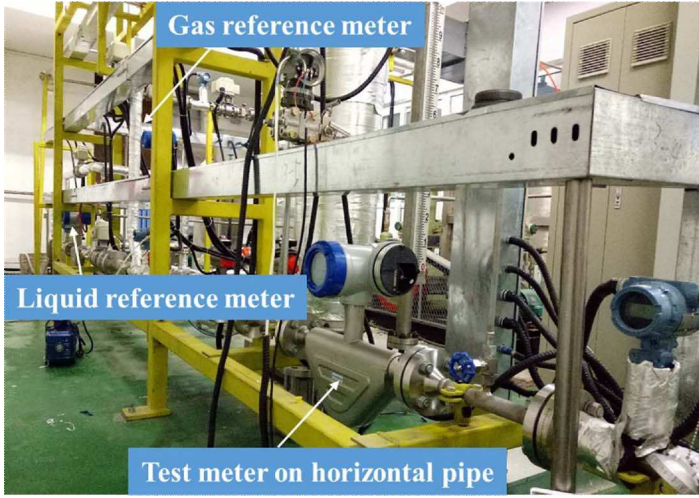
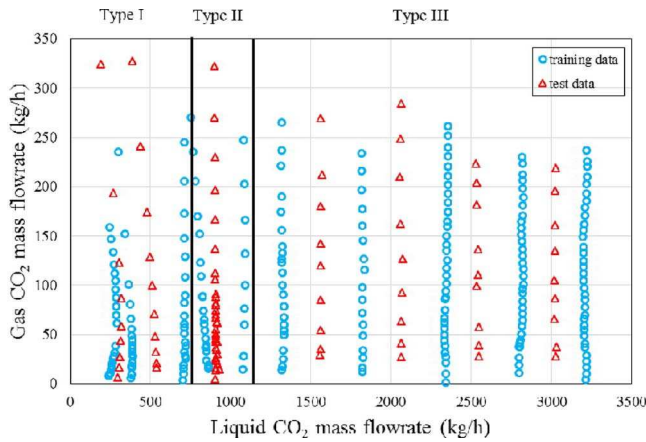**Fig. 2.** Meters under test and reference meters on the test rig.

Fig. 3. Experimental test points of gas-liquid CO_2 two-phase flow.

$$K(\mathbf{x}, x_i) = \exp\left(-\frac{\|\mathbf{x} - x_i\|^2}{2\sigma^2}\right) \tag{8}$$

The parameter σ in the RBF kernel function and the penalty parameter γ in the LSSVM model are determined by cross validation in the training process.

2.3. LSSVM model for regression

LSSVM solves the nonlinear regression problem by mapping the data into a high-dimensional feature space and then developing a linear regression model in this space (Drucker et al., 1997). Given training samples $\mathbf{X}^* = (\mathbf{x}_1, \mathbf{x}_2, ..., \mathbf{x}_n)$ and the desired output $\mathbf{y}$, the optimization problem is defined as

$$\min_{\omega,e,b} \frac{1}{2}\|\boldsymbol{\omega}\|^2 + \frac{1}{2}\gamma\sum_{i=1}^{n} e_i{}^2$$
$$\text{s.t. } y_i = \langle \boldsymbol{\omega}, \varphi(\mathbf{x}_i)\rangle + b + e_i, \quad i = 1,...,n \tag{9}$$

where γ is a penalty parameter that balances model complexity and approximation accuracy, e_i is the ith error variable and b is a bias. The Lagrangian function is determined as

$$J = \frac{1}{2}\|\boldsymbol{\omega}\|^2 + \frac{1}{2}\gamma\sum_{i=1}^{n} e_i{}^2 - \sum_{i=1}^{n} \alpha_i[\langle \boldsymbol{\omega}, \varphi(\mathbf{x}_i)\rangle + b + e_i - y_i] \tag{10}$$

where α_i ($i=1,...,n$) are the Lagrange multipliers. The conditions for optimality are given by:

$$\begin{cases} \frac{\partial J}{\partial \omega} & = 0 \rightarrow \omega = \sum_{i=1}^{n} \alpha_i \varphi(\mathbf{x}_i) \\ \frac{\partial J}{\partial b} & = 0 \rightarrow \sum_{i=1}^{n} \alpha_i = 0 \\ \frac{\partial J}{\partial e_i} & = 0 \rightarrow \alpha_i = \gamma e_i \\ \frac{\partial J}{\partial \alpha_i} & = 0 \rightarrow <\omega, \varphi(\mathbf{x}_i)> + b + e_i - y_i = 0 \end{cases} \tag{11}$$

The solutions to $\boldsymbol{\alpha}$ and b can be given in a group of linear equations by eliminating the variables $\boldsymbol{\omega}$ and e_i:

$$\begin{bmatrix} 0 & 1_v{}^T \\ 1_v & \Omega + I/\gamma \end{bmatrix} \begin{bmatrix} b \\ \boldsymbol{\alpha} \end{bmatrix} = \begin{bmatrix} 0 \\ y \end{bmatrix} \tag{12}$$

where $1_v = (1,...,1)^T$, $y = (y_1,...,y_n)^T$, $\boldsymbol{\alpha} = (\alpha_1,...,\alpha_n)^T$, $\mathbf{I}$ is an $n \times n$ identity matrix. The Mercer condition is applied:

$$\boldsymbol{\Omega}_{i,k} = <\varphi(\mathbf{x}_i), \varphi(\mathbf{x}_k)> = K(\mathbf{x}_i, \mathbf{x}_k) \ i, \quad k = 1, ...,n \tag{13}$$

Finally, the LSSVM regression model can be obtained:

$$f(\mathbf{x}) = <\omega, \varphi(\mathbf{x})> + b = \sum_{i=1}^{n} \alpha_i K(\mathbf{x}, \mathbf{x}_i) + b \tag{14}$$
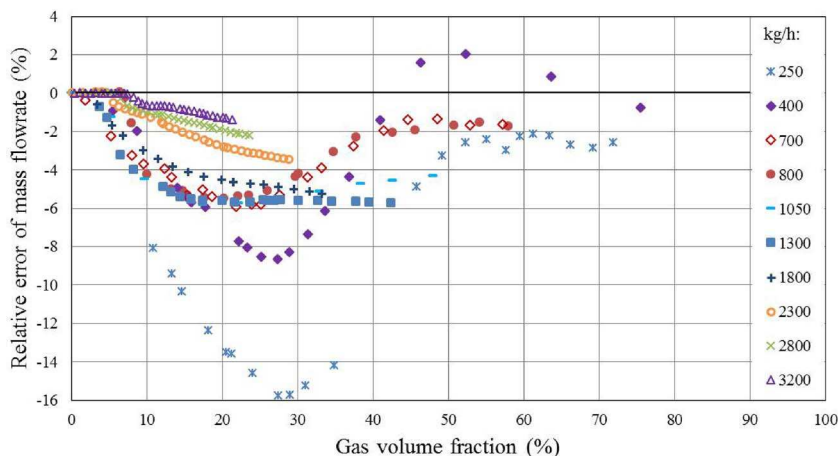
3. Experimental tests

As shown in Fig. 2, there are two independent Coriolis mass flowmeters on the liquid CO_2 flow section and gas CO_2 flow section, respectively, to provide references. The reference Coriolis flowmeters are capable of offering the CO_2 liquid measurement uncertainty of 0.16% and CO_2 gas measurement uncertainty of 0.3%. In the test section, two Coriolis flowmeters (KROHNE OPTIMASS 6400 S15) were installed in horizontal and vertical positions, respectively. These meters together with the developed data-driven models are tested with gas-liquid two-phase CO_2 flow. Different installation orientations of the Coriolis mass flowmeters are taken into account with regard to the impacts of buoyancy and gravity on mixed fluid.

In order to achieve liquid CO_2 at the single phase section and stable gas-liquid mixture at the test section, the fluid temperature was controlled between 19 °C and 21 °C through a cooling system and the pressure ranged from 54 bar to 58 bar. The liquid CO_2 mass flowrate was ranging from 250 kg/h to 3200 kg/h whilst the gas CO_2 flowrate from 0 to 330 kg/h. As acquiring a high volume of training data is not practical in addition to the potential problem of overfitting in the data-driven modelling, the training data should be representative of the whole range of data including the maximum and minimum liquid flowrates and cover the typical flow regimes to be tested. Since the error trend for stratified flow is more complicated than bubbly flow, the

(a) Horizontal orientation
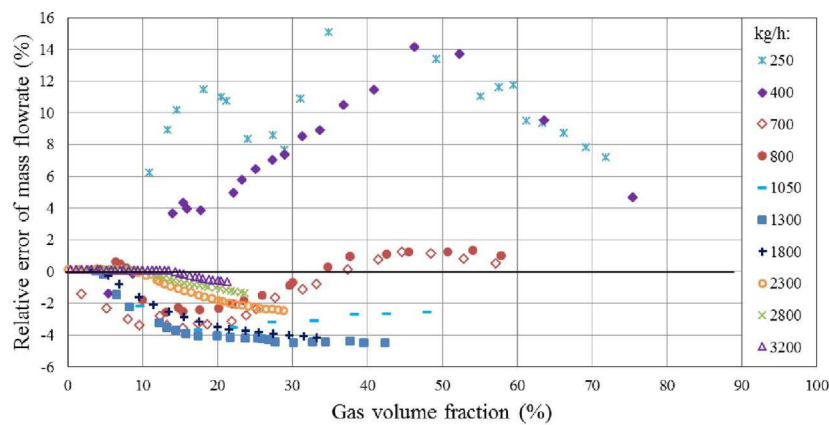
(b) Vertical orientation

Fig. 4. Original errors from Coriolis mass flowmeters.
(a) Horizontal orientation. (b) Vertical orientation.

training data for stratified flow should be collected with smaller intervals in terms of flowrates (Fig. 3) while reasonably greater intervals are applied for bubbly flow. In order to evaluate the generalization capability of the data-driven models, a set of data which are different from the training data and previously unseen by the trained data models are taken as test data. As shown in Fig. 3, the training data include 232 data sets (liquid flowrates: 250 kg/h, 400 kg/h, 700 kg/h, 800 kg/h, 1050 kg/h, 1300 kg/h, 1800 kg/h, 2300 kg/h, 2800 kg/h and 3200 kg/h) whilst 89 data sets (liquid flowrates: 300 kg/h, 550 kg/h, 900 kg/h, 1550 kg/h, 2050 kg/h, 2550 kg/h and 3050 kg/h) were taken for test purposes. The test data were acquired on the same test rig but at different liquid and gas flowrates. The environmental conditions under which the test data were collected are the same as the training data. The test matrix is divided into three types according to the flow patterns. The typical flow patterns on the horizontal pipe include stratified flow, intermittent flow and dispersed flow whilst bubbly flow, intermittent flow and dispersed flow were observed on the vertical pipe.

4. Results and discussion

4.1. Analysis of original errors

The typical original errors of the Coriolis mass flowmeters are plotted in Fig. 4. The error presented is against the liquid CO_2 mass flowrate and gas CO_2 entrainment since gas CO_2 mass flowrate cannot be ignored at higher pressure. The gas volume fraction here indicates the gas entrainment in the upstream of the tested Coriolis flowmeter. It

must be pointed out that relative error is used in this paper instead of measurement uncertainty (TUV NEL, Good Practice Guide) in order to quantify the improvement in measurement accuracy of the proposed method over the original meter output. Measurement uncertainty originates from a range of sources such as accuracy of the instrument, environmental effect, operator skills, the process of taking the measurement and fluctuations of the measurand. Combining all the uncertainty components yields the overall uncertainty in flow measurement (TUV NEL, Good Practice Guide). Since the accuracy of the instrument is the dominant component affecting the measurement uncertainty under two-phase flow conditions, this paper focuses on the accuracy evaluation of the instrument (Coriolis mass flowmeter) in terms of relative error.

As shown in Fig. 4, when the liquid flowrate is less than 800 kg/h, stratified flow can be seen from the horizontal pipe. As gas entrainment increases, the error trend goes up and generates positive errors. However, the flowmeter in vertical orientation yields smaller errors under the same conditions. From 800 kg/h to 1000 kg/h, the flow is observed as intermittent flow. As gas CO_2 increases, the two flowmeters both yield negative errors under the condition of dispersed flow. Different kinds of flow patterns present different error trends because of the inherent chaotic characteristic of gas phase distributions in the liquid phase. The installation orientation of the Coriolis flowmeter affects the bubble distribution in the Coriolis sensing tubes. The Coriolis sensing tubes, in horizontal position, are in a downward position and thus bubbles could be trapped at the inlet side with low flowrates because of the buoyancy effect. For this reason, the flow errors from Coriolis
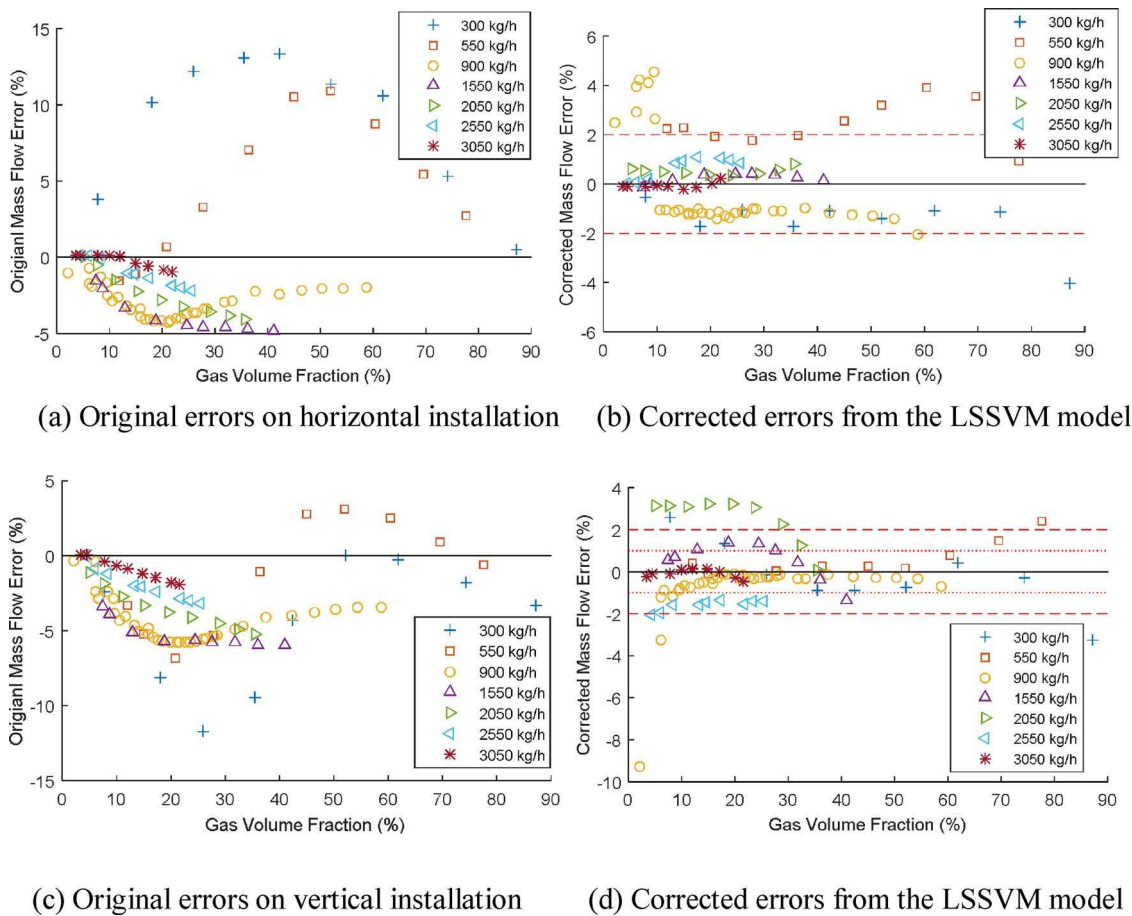
(a) Original errors on horizontal installation

(b) Corrected errors from the LSSVM model

(c) Original errors on vertical installation

(d) Corrected errors from the LSSVM model

Fig. 5. Relative errors of CO_2 mass flowrate from LSSVM models.
(a) Original errors on horizontal installation (b) Corrected errors from the LSSVM model. (c) Original errors on vertical installation (d) Corrected errors from the LSSVM model.
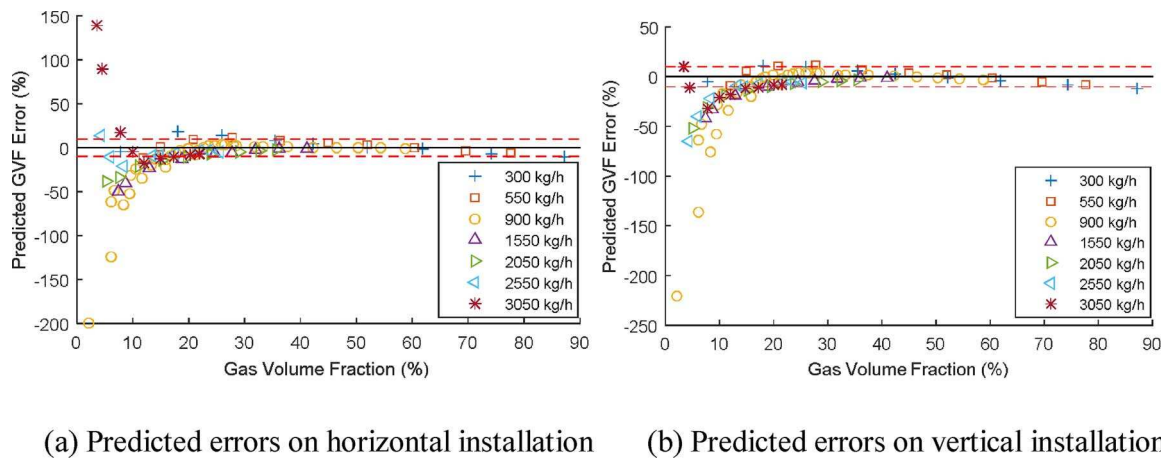

(a) Predicted errors on horizontal installation

(b) Predicted errors on vertical installation

Fig. 6. Relative errors of gas volume fraction from LSSVM models.
(a) Predicted errors on horizontal installation (b) Predicted errors on vertical installation.

flowmeters under the test conditions are positive or negative and present different trends for horizontal and vertical orientations.

4.2. LSSVM models

Two LSSVM models for the correction of the total CO_2 mass flowrate and prediction of the CO_2 gas volume fraction are developed, respectively. The models accept four variables (apparent mass flowrate, observed density, damping and DP) which are determined by input variable selection methods (Wang et al., 2017a,b). The penalty parameters

C and γ in the LSSVM models are optimized through five-fold cross validation. Through a comparison of the performances of LSSVM among four different kernel functions (including linear, polynomial, RBF and sigmoid kernel functions), the model with RBF kernel function generates the best performance. The results in the following study are from the model with RBF kernel function. The original errors and the corrected errors of CO_2 mass flowrate are depicted in Fig. 5. It can be seen that the original errors at the flowrates of 300 kg/h and 550 kg/h are very different from the rest because of the differences in flow patterns. After the correction with LSSVM models, the errors of total CO_2 mass

Table 1
Results of flow pattern recognition.

Horizontal flow patterns	Success rate	Vertical flow patterns	Success rate
Stratified flow (19)	19	Bubbly flow (19)	19
Intermittent flow (34)	34	Intermittent flow (34)	34
Dispersed flow (36)	36	Dispersed flow (36)	36
Overall success rate	100% (89/89)	Overall success rate	100% (89/89)

flowrate on horizontal and vertical pipes are significantly reduced, except that some points are overcorrected at flowrates of 900 kg/h and 2050 kg/h. Most of the corrected errors in Fig. 5 are within the ± 2% error lines.

The LSSVM prediction models for gas volume fraction takes apparent mass flowrate, observed density and DP as inputs. Fig. 6 shows that some of the errors from LSSVM models are still large, especially at the gas volume fraction less than 10%. As gas CO_2 increases, the predicted errors are all within 10% (the red dash lines in Fig. 6). Therefore, it is evident that the performance of the prediction model depends on the flow pattern, especially at the flowrates of 900 kg/h and 3050 kg/h, under which the flow is either intermittent or dispersed.

4.3. Flow pattern based LSSVM model

In order to further reduce the impact of flow patterns on the measurement from Coriolis mass flowmeters in conjunction with data-driven models, flow pattern recognition is included in the measurement system and individual correction and prediction models are developed

for individual flow patterns. Previous studies on input variable selection (Wang et al., 2017a,b) have shown that the variables, including apparent mass flowrate, observed density, damping and DP, have more significance to estimate the total CO_2 mass flowrate and CO_2 gas volume fraction which are closely related to the flow pattern. Consequently, these four variables are taken as inputs to the flow pattern recognition model. An LSSVM based flow pattern recognition model is developed to act as the flow pattern classifier. For test purposes, there are 19 data indicating stratified flow in the horizontal pipe and bubbly flow in the vertical pipe, respectively, 34 data from intermittent flow and 36 data from dispersed flow on both horizontal and vertical pipes, respectively. The results of flow pattern recognition are summarised in Table 1. Due to the high performance of LSSVM for classification, all the test points are correctly classified into the corresponding flow patterns and result in 100% successful recognition rate.

Once the test point is classified into a specific flow pattern, the corresponding correction and prediction models are determined to yield the corrected CO_2 mass flowrate and predicted gas volume fraction. The corrected errors of the total CO_2 mass flowrate are shown in Fig. 7. The red, green and blue markers represent the test points from Types I, II and III, respectively. It is obvious that the test points at Types II and III are all within ± 2% for the horizontal installation and ± 1% for the vertical installation. Meanwhile, the errors of mass flowrate at Type I are largely reduced in comparison with the results from the LSSVM models. The maximum errors at low flowrates are all within ± 5%. The correction model for mass flow measurement on the vertical installation outperforms the horizontal one at the flowrates of 300 kg/h and 550 kg/h and results in relative errors within ± 2%.

The relative errors of gas volume fraction from the flow pattern based LSSVM models are plotted in Fig. 8. Although the errors are still
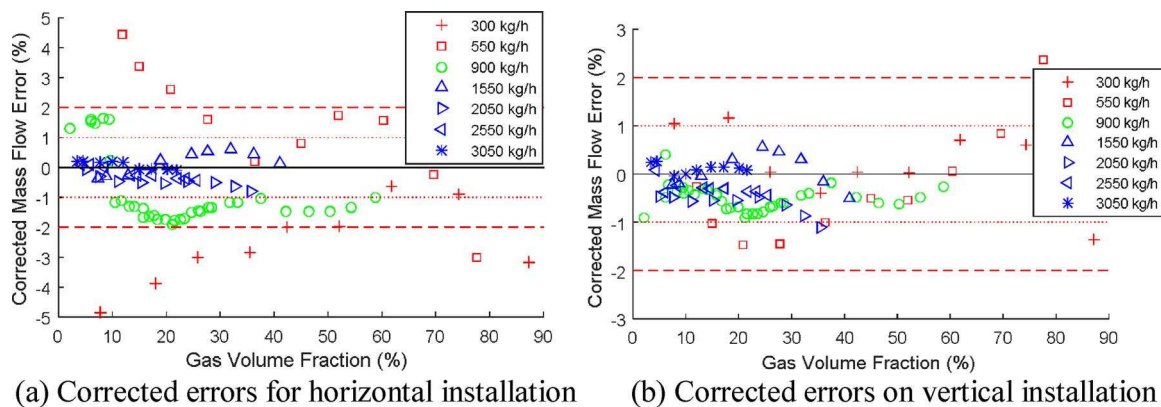

(a) Corrected errors for horizontal installation   (b) Corrected errors on vertical installation

Fig. 7. Relative errors of CO_2 mass flowrate from FP_LSSVM model.
(a) Corrected errors for horizontal installation (b) Corrected errors on vertical installation.

(a) Predicted errors on horizontal installation   (b) Predicted errors on vertical installation
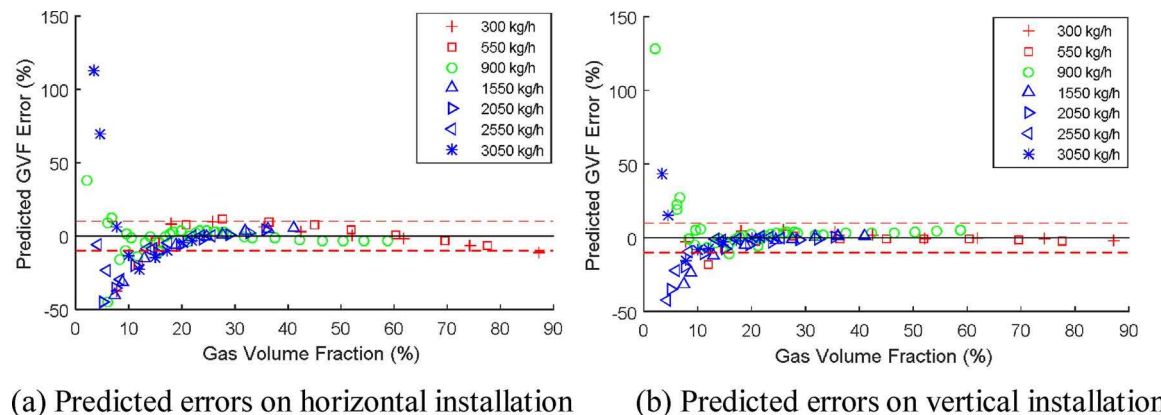
Fig. 8. Relative errors of gas volume fraction from FP_LSSVM model.
(a) Predicted errors on horizontal installation (b) Predicted errors on vertical installation.

Table 2

NRMSE comparison of BP-ANN, LSSVM and FP_LSSVM models.

NRMSE (%)	Original	LSSVM	FP_LSSVM
$CO_2\_M\_H$	2.82	1.05	0.80
$CO_2\_M\_V$	3.69	1.77	0.51
$CO_2\_G\_H$	–	10.24	8.11
$CO_2\_G\_V$	–	10.49	4.32

large at the CO_2 gas volume fraction lower than 5%, the errors at other test points are within ± 10%.

4.4. Results comparison

NRMSE results from the LSSVM and flow pattern based LSSVM (FP_LSSVM) models are summarized in Table 2. $CO_2\_M\_H$ and $CO_2\_M\_V$ present the correction models of mass flowrate. Likewise, $CO_2\_G\_H$ and $CO_2\_G\_V$ indicate the prediction models of gas volume fraction on horizontal and vertical sections, respectively. The errors of total CO_2 mass flowrate have been significantly reduced with the use of correction models. For the Coriolis mass flowmeter in horizontal orientation, NRMSE is reduced from 2.82% to 1.05% and 0.80% by using LSSVM model and FP_LSSVM model, respectively. Meanwhile, for the Coriolis mass flowmeter in vertical orientation, NRMSE is reduced from 3.69% to 1.77% and 0.51% with LSSVM and FP_LSSVM models, respectively. Moreover, the NRMSEs from the FP_LSSVM models are much smaller than the LSSVM models for both installation orientations.

As for the estimation of CO_2 gas volume fraction, the results from the models demonstrate that the FP_ LSSVM models also outperform the LSSVM models. The NRMSEs from the LSSVM models are around 10% while those from the FP_LSSVM models are 8.11% and 4.32% for horizontal and vertical installations, respectively.

5. Conclusions

The performance of Coriolis flowmeters with flow pattern based LSSVM models has been assessed with gas-liquid two-phase CO_2 flow. A range of experimental tests were conducted on a gas-liquid two-phase CO_2 test rig. Experimental results have demonstrated that the relative errors from Coriolis mass flowmeters in conjunction with the correction models are mostly within ± 2% in horizontal installation and ± 1.5% in vertical position for flowrates ranging from 250 kg/h to 3200 kg/h. The proposed measurement system has shown significant improvement for the measurement of gas-liquid CO_2 flow. The predicted errors of gas volume fraction are no greater than ± 10% over the same range of flowrates with GVF down to less than 5%. In comparison with the LSSVM models, the flow pattern based LSSVM models have produced much smaller errors in the prediction of gas volume fraction. The results presented have confirmed that the applicability of Coriolis flowmeters to single-phase CO_2 flow measurement has been effectively extended to two-phase CO_2 flow metering under CCS conditions.

References

Adefila, K., Yan, Y., Sun, L., Wang, T., 2015. Calibration of an averaging pitot tube for gaseous CO_2 flowmetering. IEEE Trans. Instrum. Meas. 64, 1240–1249.

Adefila, K., Yan, Y., Sun, L., Wang, T., 2017. Flow measurement of wet CO_2 using an averaging pitot tube and coriolis mass flowmeters. Int. J. Greenh. Gas Control 63, 289–295.

Cortes, C., Vapnik, V., 1995. Support-vector network. Mach. Learn. 20, 273–297.

Drucker, H., Burges, C., Kaufman, L., Smola, A., Vapnik, V., 1997. Support vector regression machines. Neural Inf. Process. Syst. 9, 155–161.

Green, T., Reese, M., Henry, M., 2008. Two-phase CO_2 measurement and control in the Yates oil field. Meas. Control 41, 205–207.

Hemp, J., Sultan, G., 1989. On the theory and performance of Coriolis mass flowmeters. International Conference on Mass flow measurement 1–38.

Hou, Q., Xu, K., Fang, M., Shi, Y., Tao, B., Jiang, R., 2014. Gas-liquid two-phase flow correction method for digital CMF. IEEE Trans. Instrum. Meas. 63, 2396–2404.

Huang, G., Zhou, H., Ding, X., Zhang, R., 2012. Extreme learning machine for regression and multiclass classification. IEEE Trans. Syst. Man Cybern. B 42, 513–529.

Hunter, L., Leslie, G., 2009. National physical laboratory (NPL): A study of measurement issues for carbon capture and storage (CCS). TUV NEL Ltd, Glasgow, U.K., Tech. Rep. 2009/54.

Kunze, J.W., Storm, R., Wang, T., 2014. Coriolis mass flow measurement with entrained gas. Sensors and Measuring Systems, Nuremberg, Germany, 3-4 June 1–6.

Lin, C., Bhattacharji, A., Spicer, G., Maroto-Valer, M., 2014. Coriolis metering technology for CO_2 transportation for carbon capture and storage. Energy Procedia 63, 2723–2726.

Liu, R., Fuent, M., Henry, M., Duta, M., 2001. A neural network to correct mass flow errors caused by two-phase flow in a digital Coriolis mass flowmeter. Flow Meas. Instrum. 12, 53–63.

TUV NEL, 2009. Measurement of CO2 throughout the carbon capture and storage (CCS) chain. [23/11/2017]. Available from: http://www.tuvnel.com/_x90lbm/ Measurement_of_CO2_Throughout_the_Carbon_Capture_and_Storage_CCS_Chain.pdf.

TUV NEL, Good Practice Guide. Flow measurement uncertatinty and data reconciliation. [23/11/2017]. Available from: http://www.tuvnel.com/_x90lbm/Flow_ Measurement_Uncertainty_and_Data_Reconciliation.pdf.

Safarinejadian, B., Tajeddini, M., Mahmoodi, L., 2012. A new fuzzy based method for error correction of Coriolis mass flow meter in presence of two-phase fluid. In: International Conference on Artificial Intelligence and Image Processing. Dubai, UAE, 6-7 October. pp. 192–196.

Suykens, J.A.K., Vandewalle, J., 1999. Least squares support vector machine classifiers. Neural Process. Lett. 9, 293–300.

Wang, L., Liu, J., Yan, Y., Wang, X., Wang, T., 2017a. Gas-liquid tow-phase flow measurement using Coriolis flowmeters incorporating articial neural networks, support vector machine and genetic programming algorithms. IEEE Trans. Instrum. Meas. 66, 852–868.

Wang, L., Yan, Y., Wang, X., Wang, T., 2017b. Input variable selection for data-driven models of Coriolis flowmeters for two-phase flow measurement. Meas. Sci. Technol. 28, 1–12.

Wang, T., Baker, R., 2014. Coriolis flowmeters: a review of developments over the past 20 years, and an assessment of the state of the art and likely future directions. Flow Meas. Instrum. 40, 99–123.

Xing, L., Geng, Y., Hua, C., Zhu, H., Rieder, A., 2014. A combination method for metering gas-liquid two-phase flows of low liquid loading applying ultrasonic and Coriolis flowmeters. Flow Meas. Instrum. 37, 135–143.